9708 *Biochemistry* **2009,** *48,* 9708–9710
DOI: 10.1021/bi9008787

BIOCHEMISTRY
including biophysical chemistry & molecular biology
Rapid Report

A General and Efficient Approach for NMR Studies of Peptide Dynamics in Class I MHC Peptide Binding Grooves[†]

Francis K. Insaidoo, Jaroslav Zajicek, and Brian M. Baker*

Department of Chemistry and Biochemistry and Walther Cancer Research Center, 251 Nieuwland Science Hall, University of Notre Dame, Notre Dame, Indiana 46556

Received May 24, 2009; Revised Manuscript Received August 14, 2009

ABSTRACT: T-Cell receptor recognition of peptides bound by major histocompatibility complex (MHC) proteins initiates a cellular immune response. Dynamics of peptides within MHC binding grooves can influence TCR recognition, yet NMR studies which could address this rigorously have been hindered by the expense of isotopically labeled peptides and the large size of peptide−MHC complexes. Here we describe a methodology for characterizing peptide dynamics within MHC binding grooves via NMR, using a biosynthetic approach for producing labeled peptide. With the Tax_{11-19} peptide bound to the human class I MHC HLA-A*0201, we demonstrate that peptide generated in this manner can be well characterized in MHC binding grooves by NMR, providing opportunities to more precisely study the role of peptide dynamics in TCR recognition. Demonstrating the utility of such studies, the data with the Tax_{11-19} peptide indicate the presence of slow conformational exchange in the peptide, supporting an "induced-fit" style TCR binding mechanism.

Recognition of peptides bound and presented by major histocompatibility complex proteins (pMHC)[1] by T-cell receptors (TCR) on cytotoxic or helper T-cells initiates a signaling cascade leading to a cellular immune response. TCRs on cytotoxic T-cells recognize a composite surface formed by the peptide and the α_1 and α_2 helices of the class I MHC protein. TCR specificity toward different pMHC ligands is usually attributed to conformational differences between the bound peptides (*1*), yet emerging data indicate that peptide flexibility within the MHC peptide binding groove can dramatically influence TCR recognition. For example, we recently demonstrated that modifications of the position 2 anchor residue of the Melan-A/MART-1_{27-35} tumor antigen result in enhanced peptide dynamics in the MHC peptide groove and a loss of recognition by antigen-specific T-cells (*2*). As there is growing interest in utilizing the T-cell arm of the immune system for the development of vaccines, therapeutic interventions, and imaging reagents, the potential influence of molecular motion in immune recognition, specificity, and cross-reactivity is significant.

Although crystallography, molecular dynamics simulations, infrared spectroscopy, and time-resolved fluorescence anisotropy have been used to examine dynamics of peptides bound to class I MHC molecules (*2*−*4*), nuclear magnetic resonance (NMR) relaxation techniques should be expected to provide advantages over these techniques because of their ability to resolve residue-specific molecular motions across a range of time scales without the need for an exogenous label. However, NMR studies of peptides in MHC binding grooves have been hindered by the prohibitive cost of isotopically labeled peptides and the large size (∼45 kDa) of the pMHC complex.

Here, we describe the methodology for characterizing the dynamics of peptides in class I MHC peptide binding grooves via NMR using biosynthetic labeled peptides. Although other systems have been described for the biological expression of labeled peptides, a drawback of most is the fact that the peptide contains chemically modified or additional amino acids at the N- or C-terminus. Such approaches are suboptimal for producing peptides for incorporation into class I MHC molecules given the length restrictions and requirement for defined N- and C-termini.

To overcome these limitations, we adapted a method in which the peptide of interest was fused to the C-terminus of ubiquitin, in turn modified with an N-terminal hexahistidine tag (*5*, *6*). Ubiquitin is frequently used in the development of NMR methods, and well-developed protocols exist for the expression of large quantities of isotopically labeled protein in bacterial systems (*7*). For cleavage of the peptide from ubiquitin, we used the ubiquitin hydrolase YUH 1, likewise modified with a C-terminal histidine tag. As YUH 1 cleaves the peptide bond immediately after the terminal glycine of ubiquitin using only the final five ubiquitin amino acids for substrate recognition (*8*), there are few restrictions on the sequence of the fused peptide, and once cleaved, the peptide is available unmodified. Further, as both the fusion protein and hydrolase possess histidine tags, purification of both proteins and separation of ubiquitin and the hydrolase from the cleaved peptide are straightforward.

As a demonstration system, we used the Tax_{11-19} peptide (Tax, LLFGYPVYV) bound to the class I MHC molecule HLA-A*0201 (HLA-A2). The Tax peptide is bound by HLA-A2 in the usual extended conformation (*9*) but undergoes a large conformational change when the Tax−HLA-A2 complex is recognized by the A6 and B7 TCRs (*10*). The change is centered at the backbones of Pro6 and Val7, and although it is consistent with an induced-fit mechanism, it is possible the conformational change is facilitated by conformational selection due to rapid dynamics in the unligated pMHC molecule. NMR dynamics studies of the Tax peptide bound to HLA-A2 can help elucidate the extent to which dynamics contributes to the structurally observed conformational change.

[†]Supported by the National Science Foundation (Grant MCB-0338298 to B.M.B.). F.K.I. was supported by the Notre Dame CBBI training program, funded by Grant T32GM075762 from the National Institute of General Medical Sciences, National Institutes of Health.

*To whom correspondence should be addressed. E-mail: brian-baker@nd.edu. Phone: (574) 631-9810. Fax: (574) 631-6652.

[1]Abbreviations: MHC, major histocompatibility complex; pMHC, peptide−MHC complex; TCR, T-cell receptor; CDR, complementarity-determining region.

 Published on Web 09/17/2009

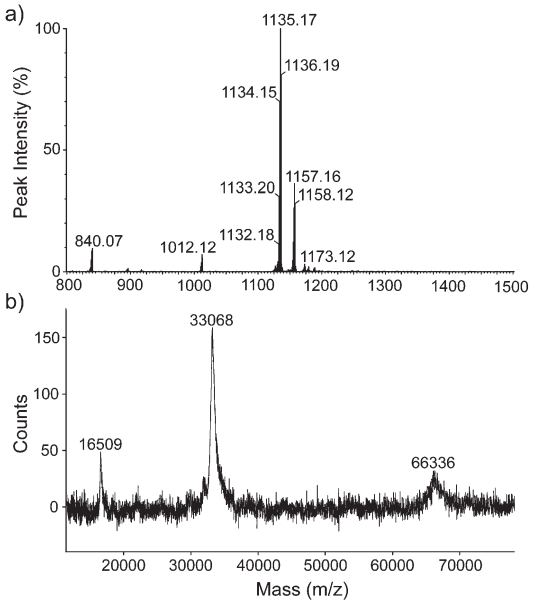

FIGURE 1: Isotopic labeling of the Tax peptide and the HLA-A2 heavy chain. (a) Mass spectral analysis of the purified biosynthetic ^{13}C- and ^{15}N-labeled Tax peptide indicates near-complete labeling. The calculated molecular mass of uniformly labeled Tax peptide is 1135 Da, whereas that of the unlabeled peptide is 1070 Da (the peak at 1157 Da represents a sodium adduct). (b) MALDI-TOF mass spectral analysis of deuterated HLA-A2 heavy chain shows a strong peak at 33068 Da. The molecular mass of the unlabeled heavy chain is 31930 Da, indicating approximately 98% deuteration.

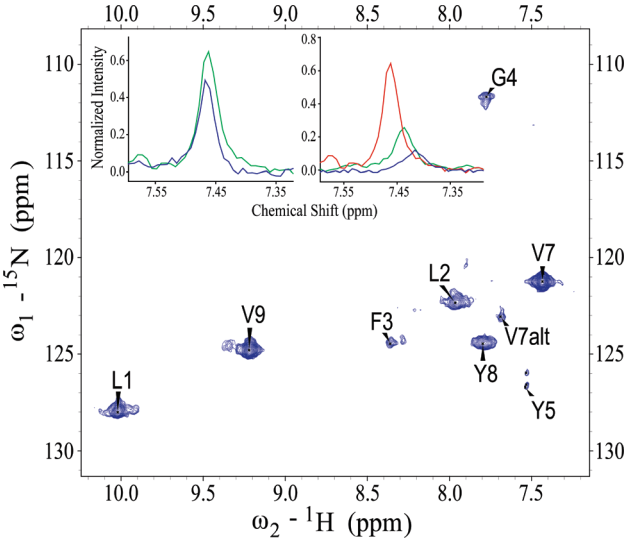

FIGURE 2: Two-dimensional $^{1}H-^{15}N$ TROSY-HSQC spectrum of [^{13}C,^{15}N]Tax bound to HLA-A2. Data were acquired on a Bruker Avance 800 MHz (18.8 T) spectrometer in 20 mM [^{2}H]bis-tris with [^{2}H]benzoic acid (pH 7.4), 90% H_2O, and 10% $^{2}H_2O$ at 37 °C. V7alt indicates a weak, alternate peak for Val7. The left inset indicates signal enhancement for the major Val7 peak from deuteration of the HLA-A2 heavy chain and use of a deuterated, low-conductivity buffer. The right inset shows the temperature dependence of the signal strength for the major Val7 peak: 25 (blue), 35 (green), and 45 °C (red).

For generating isotopically labeled Tax peptide, the ubiquitin−peptide fusion protein and YUH 1 were expressed separately in *Escherichia coli* BL21(DE3) cells grown in either rich medium for YUH 1 or minimal M9 medium supplemented with [^{15}N]$(NH_4)_2SO_4$ and/or [^{13}C]glucose for the ubiquitin−peptide fusion. Three to six hours after induction, cells were harvested. Enrichment of the protein followed commercial protocols. After Ni-NTA affinity column purification, further purification was achieved using size exclusion chromatography. Yields were approximately 40−60 mg of ubiquitin−peptide fusion protein per liter of cells and 90−120 mg of YUH 1 per liter of cells. β-Mercaptoethanol was added to the YUH 1 preparation to a final concentration of 5 mM, and the peptide was cleaved using a 30% YUH 1:ubiquitin molar ratio in 500−2000 μL reaction mixtures at 37 °C for 6 h. Cleaved peptide was purified from the reaction mixture via a second round of Ni-NTA followed by size exclusion chromatography. Final yields of >99% ^{13}C- and ^{15}N-labeled peptide were approximately 6−10 mg per liter of cells. Peptide identity and labeling were verified by LC−MS (Figure 1A).

The method outlined above facilitates rapid and straightforward expression of labeled peptides, yet for the performance of NMR on pMHC complexes, the complexity of the large protein remains. To help overcome this, the heavy chain of the HLA-A2 complex was deuterated to approximately 98% by bacterial expression of the heavy chain in M9 medium (*11*, *12*) supplemented with 3 g/L [^{2}H]Celtone base powder (Figure 1B). Inclusion body preparation and refolding of the deuterated heavy chain and protonated β_2-microglobulin subunit in the presence of ^{13}C- and ^{15}N-labeled peptide then followed the normal procedure for production of class I pMHC complexes (*13*). Coupled with the use of a deuterated, low-conductivity buffer (*14*), heavy chain deuteration improved the NMR signal by ~50%.

Figure 2 shows a two-dimensional $^{1}H-^{15}N$ TROSY-HSQC spectrum for Tax bound to HLA-A2 collected at 37 °C on a 18.8 T spectrometer with a cryogenic probe. Insets illustrate the signal enhancement due to heavy chain deuteration as well as exploration of the signal temperature dependence. An experimental temperature of 37 °C was chosen as a trade-off between the increased sensitivity available at higher temperatures and the stability of the pMHC complex. Although the T_m of the Tax−HLA-A2 complex is near 65 °C (*9*), other pMHC complexes of lower stability may necessitate lower temperatures for data acquisition.

Assignments for the data shown in Figure 2 were achieved using HCCH-TOCSY, HCACO, HNCO, and HSQC experiments (*15*−*21*). Multiple peaks were identified for Val7, possibly reflecting the sampling on a slow time scale of alternate conformations, one of which may correspond to the TCR-bound state in the unligated pMHC complex. The identities of the Val7 peaks were confirmed with a control experiment with the Tax−HLA-A2 complex in which the Tax peptide had been prepared via solid-phase synthesis with ^{15}N-labeled valine at position 7.

A saturation transfer experiment was used to examine conformational exchange occurring between the two peaks observed for Val7. When the main peak near 7.5 ppm was irradiated with a saturation time of 2.5 s, no changes were observed in the alternate peak at 7.8 ppm, confirming slow exchange on the NMR time scale.

To demonstrate the capacity to explore peptide dynamics via NMR, we measured ^{15}N longitudinal (R_1) and rotating-frame ($R_{1\rho}$) relaxation rates for all residues of the Tax peptide (excluding Pro6). The resulting rates are summarized in Figure 3 (accurate relaxation data could only be determined for the predominant Val7 peak). Although there is variation across the peptide, it is interesting that the rates in the center of the peptide

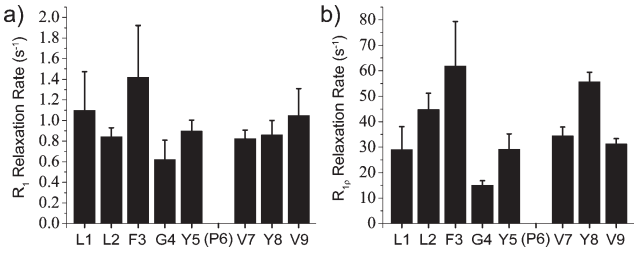

FIGURE 3: Longitudinal (A) and rotating-frame (B) relaxation rates for [^{13}C,^{15}N]Tax peptide bound to HLA-A2 reveal differential dynamics across the bound peptide.

are relatively low, particularly when considering that positions 2 and 9 are primary anchor residues whose side chains are "pinned down" within the peptide binding groove. The centers of antigenic peptides are commonly thought to be the "focus" of the hypervariable CDR3 loops of TCRs (*22*), and reduced flexibility at the center of the peptide may reflect this. The relatively low rates for Val7 are consistent with the HSQC and saturation transfer experiments indicating slow conformational exchange and suggest that any sampling of the TCR-bound conformation in the unligated pMHC likewise occurs on a slow time scale.

To follow up on the dynamical behavior for Val7, we examined the flexibility of the Tax peptide bound to HLA-A2 by molecular dynamics (MD) simulations, using an unrestrained MD protocol we recently employed with the MART-1/Melan-A tumor antigen (*2*). Over the course of a 30 ns simulation at 300 K, the backbone of Val7 populated two distinct conformations, with the crystallographically observed conformation populated 85% of the time and an alternative conformation that has not been observed in any structure populated 15% of the time (Figure S3A of the Supporting Information). Increasing the simulation temperature to 330 K decreased the percentage of the unligated conformation to 81%. Notably though, at the elevated temperature, the TCR-bound conformation was populated only 2% of the time (Figure S3B of the Supporting Information). These observations are consistent with two predictions from the NMR data. The first is the existence of multiple peptide conformations separated by high barriers, particularly for Val7. The second is that the conformational change around Pro6/Val7 that occurs upon binding of the A6 and B7 TCRs may reflect more of an "induced-fit" style binding mechanism rather than a mechanism based on conformational selection in the unbound pMHC.

In summary, we have demonstrated a methodology for collecting high-resolution NMR data on peptides bound within class I MHC peptide binding grooves. The approach is entirely general and can be easily adapted to different peptides and MHC molecules. As demonstrated with the Tax peptide, application of this approach can be expected to help reveal the influence peptide molecular motion has in T-cell recognition of the antigen. Given the growing appreciation for the role of molecular flexibility in influencing TCR recognition of pMHC (*23*), as well as the expanding interest in the development of peptide/MHC-based vaccines, therapeutic agents, and imaging tools, NMR characterizations of peptide dynamics should have a significant impact in both basic and applied immunology.

ACKNOWLEDGMENT

We thank Dr. Jeffrey Peng for helpful advice and Dr. Kenneth P. Murphy for kindly providing expression vectors for ubiquitin and the YUH 1 hydrolase.

SUPPORTING INFORMATION AVAILABLE

Expanded methods, R_1 and $R_{1\rho}$ analyses, and MD simulation results. This material is available free of charge via the Internet at http://pubs.acs.org.

REFERENCES

1. Madden, D. R. (1995) *Annu. Rev. Immunol. 13*, 587–622.
2. Borbulevych, O. Y., Insaidoo, F. K., Baxter, T. K., Powell, D. J.Jr., Johnson, L. A., Restifo, N. P., and Baker, B. M. (2007) *J. Mol. Biol. 372*, 1123–1136.
3. Pohlmann, T., Bockmann, R. A., Grubmuller, H., Uchanska-Ziegler, B., Ziegler, A., and Alexiev, U. (2004) *J. Biol. Chem. 279*, 28197–28201.
4. Fabian, H., Huser, H., Narzi, D., Misselwitz, R., Loll, B., Ziegler, A., Bockmann, R. A., Uchanska-Ziegler, B., and Naumann, D. (2008) *J. Mol. Biol. 376*, 798–810.
5. Kohno, T., Kusunoki, H., Sato, K., and Wakamatsu, K. (1998) *J. Biomol. NMR 12*, 109–121.
6. Mildner, A. M., Paddock, D. J., LeCureux, L. W., Leone, J. W., Anderson, D. C., Tomasselli, A. G., and Heinrikson, R. L. (1999) *Protein Expression Purif. 16*, 347–354.
7. Fiaux, J., Bertelsen, E. B., Horwich, A. L., and Wuthrich, K. (2004) *J. Biomol. NMR 29*, 289–297.
8. Johnston, S. C., Riddle, S. M., Cohen, R. E., and Hill, C. P. (1999) *EMBO J. 18*, 3877–3887.
9. Khan, A. R., Baker, B. M., Ghosh, P., Biddison, W. E., and Wiley, D. C. (2000) *J. Immunol. 164*, 6398–6405.
10. Ding, Y. H., Smith, K. J., Garboczi, D. N., Utz, U., Biddison, W. E., and Wiley, D. C. (1998) *Immunity 8*, 403–411.
11. Marley, J., Lu, M., and Bracken, C. (2001) *J. Biomol. NMR 20*, 71–75.
12. Cai, M. L., Huang, Y., Sakaguchi, K., Clore, G. M., Gronenborn, A. M., and Craigie, R. (1998) *J. Biomol. NMR 11*, 97–102.
13. Garboczi, D. N., Hung, D. T., and Wiley, D. C. (1992) *Proc. Natl. Acad. Sci. U.S.A. 89*, 3429–3433.
14. Kelly, A. E., Ou, H. D., Withers, R., and Dotsch, V. (2002) *J. Am. Chem. Soc. 124*, 12013–12019.
15. Kay, L. E., Ikura, M., Tschudin, R., and Bax, A. (1990) *J. Magn. Reson. 89*, 496–514.
16. Kay, L. E., Keifer, P., and Saarinen, T. (1992) *J. Am. Chem. Soc. 114*, 10663–10665.
17. Kay, L. E., Xu, G. Y., Singer, A. U., Muhandiram, D. R., and Formankay, J. D. (1993) *J. Magon. Reson., Ser. B 101*, 333–337.
18. Bodenhausen, G., and Ruben, D. J. (1980) *Chem. Phys. Lett. 69*, 185–189.
19. Piotto, M., Saudek, V., and Sklenar, V. (1992) *J. Biomol. NMR 2*, 661–665.
20. Sklenar, V., Piotto, M., Leppik, R., and Saudek, V. (1993) *J. Magon. Reson., Ser. A 102*, 241–245.
21. Salzmann, M., Pervushin, K., Wider, G., Senn, H., and Wuthrich, K. (1998) *Proc. Natl. Acad. Sci. U.S.A. 95*, 13585–13590.
22. Garboczi, D. N., and Biddison, W. E. (1999) *Immunity 10*, 1–7.
23. Armstrong, K. M., Piepenbrink, K. H., and Baker, B. M. (2008) *Biochem. J. 415*, 183–196.